

Static behavior of stud shear connectors with initial damage in steel-UHPC composite bridges

Jianan Qi^{*1}, Yiqun Tang^a, Zhao Cheng^b, Rui Xu^c and Jingquan Wang^d

Key Laboratory of Concrete and Prestressed Concrete Structures of the Ministry of Education, School of Civil Engineering, Southeast University, Nanjing, China

(Received December 1, 2019, Revised February 15, 2020, Accepted February 17, 2020)

Abstract. For steel-concrete girders made composite using shear studs, initial damage on studs induced by weld defect, unexpected overloading, fatigue and others might degrade the service performance and even threaten the structural safety. This paper conducted a numerical study to investigate the static behavior of damaged stud shear connectors that were embedded in ultra high performance concrete (UHPC). Parameters included damage degree and damage location. The material nonlinear behavior was characterized by multi-linear stress-strain relationship and damage plasticity model. The results indicated that the shear strength was not sensitive to the damage degree when the damage occurred at $2/3d$ (d is the stud diameter) from the stud root. An increased stud area would be engaged in resisting shear force as the distance of damage location from stud root increased and the failure section becomes inclined, resulting in a less reduction in the shear strength and shear stiffness. The reduction factor was proposed to consider the degradation of the shear strength of the damaged stud. The reduction factor can be calculated using two approaches: a linear relationship and a square relationship with the damage degree corresponding to the shear strength dominated by the section area and the nominal diameter of the damaged stud. It was found that the proposed method is preferred to predict the shear strength of a stud with initial damage.

Keywords: composite bridges; stud shear connector; ultra high performance concrete (UHPC); initial damage; shear strength; finite element analysis

1. Introduction

Ultra high performance concrete (UHPC) is an advanced cementitious material with superior mechanical properties and excellent durability (De Larrard and Sedran 1994, Qi *et al.* 2018a, Sharma and Bansal 2019). Due to the randomly dispersed high strength steel fibers and fiber bridging effect, UHPC exhibits high tensile strength, ultimate tensile strain, strain-hardening behavior, and high crack resistance (Mosaberpanah and Eren 2017, Qi *et al.* 2017a, Qi *et al.* 2018b, Qi *et al.* 2019b).

Recently, UHPC has been introduced to the steel-concrete composite bridges to prevent the concrete slab cracking problem (Kim *et al.* 2015, Cao *et al.* 2017, Wang *et al.* 2017). Many researches have verified the constructability and superiority of such steel-UHPC composite bridges (Shao *et al.* 2018, Liu *et al.* 2019). However, damage to stud shear connectors may induced by weld defect, unexpected overloading, fatigue and other factors, which has been detected in existing composite bridges (Qi *et al.* 2017b). Initial damage on studs might

degrade the service performance and even threaten the safety and service life of composite bridges, reducing the benefits of UHPC slab. Therefore, reliability assessment on the shear behavior of damaged stud shear connectors is necessary for popularizing of UHPC-steel composite bridges in engineering practice.

Numerous studies have been conducted to investigate the shear behavior of studs that are embedded in UHPC. Wang *et al.* (2019) carried out an experimental study on the large stud shear connectors in UHPC and found that UHPC matched well with large studs. Kruszewski *et al.* (2018) evaluated the push-out behavior of stud shear connectors welded on thin plates and embedded in UHPC and pointed out that this repair method could be used for steel bridge girders with damage at the ends. Qi *et al.* (2019a) performed an experimental and numerical investigation on the static behavior of stud shear connectors in UHPC. They found that the shear strength is supposed to be composed of two parts stud shank shear contribution and concrete wedge block shear contribution. Wang *et al.* (2017) performed a series of tests on demountable headed stud shear connectors in steel-UHPC composite structures. They found that tensile failure due to UHPC breakout could occur if the stud aspect ratio was less than 1.5. Based on the results, Cao *et al.* (2017) showed that the short-headed studs therefore could develop full strength in UHPC. Kim *et al.* (2015) demonstrated that the aspect ratio could be reduced from 4 to 3.1 without loss of shear strength and no splitting crack occurred at the UHPC slab. Rauscher and Hegger (2008) investigated the static behavior of continuous shear

*Corresponding author, Assistant Professor

E-mail: qijianan723@126.com

^aAssociate Professor

^bPostdoctoral Fellow

^cPh.D. Student

^dProfessor

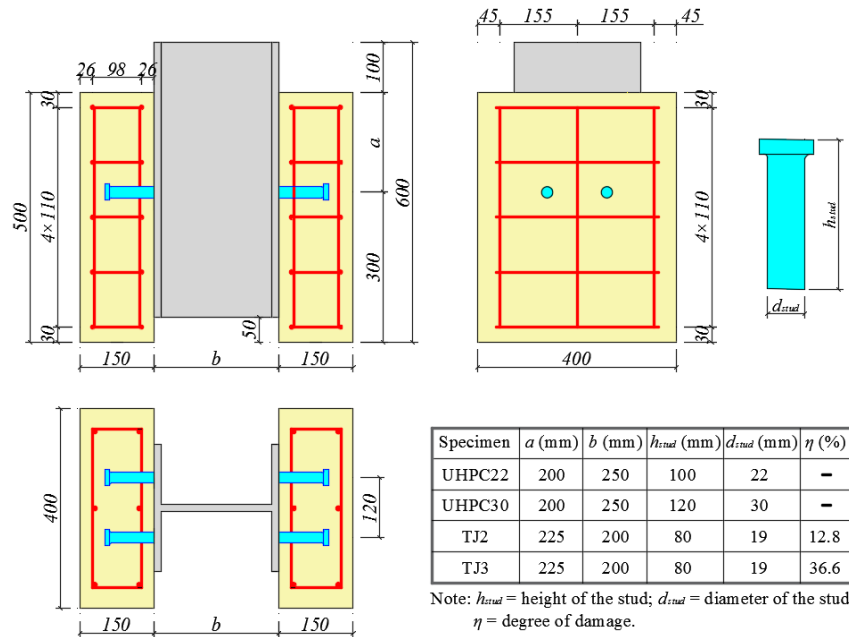


Fig. 1 Specimen details and test parameters (unit: mm)

connectors in UHPC and found that continuous shear connectors were capable of transferring high shear forces in UHPC. However, limited researches can be found in literature regarding the shear behavior of studs shear connectors with initial damage in concrete slab. Qi *et al.* (2017b) experimentally and numerically studied the shear behavior of stud shear connectors with initial damage embedded in normal strength concrete and proposed a reduction factor to consider the reduction of the shear strength due to initial damage. By using a numerical simulation, Xu and Sugiura (2013) pointed out that flexural bending acting on the concrete slabs caused a reduction in the stud shear stiffness but had no significant influence on the shear strength. Oehlers and Park (1992) noted that the initial damage of the longitudinal cracks on the concrete slabs reduced the shear strength of the associated shear connectors. It can be concluded that no public report to date has been specifically focused on the shear behavior of stud shear connectors with initial damage embedded in UHPC.

This study focused on the effect of initial damage on the static behavior of stud shear connectors in steel-UHPC composite bridges. A finite element (FE) model was developed for stud shear connectors with initial damage using general commercial software ABAQUS. The accuracy of the FE model was validated using the reported test results. The effect of damage degree and damage location on the shear behavior of initial damaged studs was investigated based on the proposed FE model. A theoretical formula supplemented with a reduction factor K was proposed to consider the reduction of the shear strength due to the initial damage and was verified using FE calculation results.

2. Finite element model

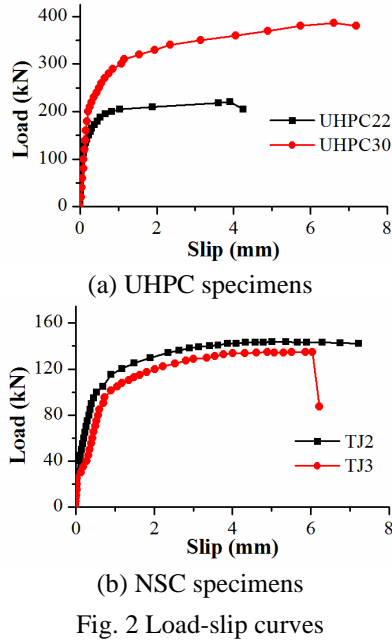
Although some experimental studies have been

conducted on the shear behavior of stud shear connectors embedded in UHPC slabs, no public report has been specially focused on the shear behavior of stud shear connectors with initial damage embedded in UHPC slabs. In addition, limited test data can be found regarding the push-out test results of stud shear connectors with initial damage in normal strength concrete (NSC). It is inferred that if a FE model can simultaneously simulate the shear behavior of studs in UHPC and studs with initial damage in NSC, it is believed that the proposed FE model could simulate the shear behavior of studs with initial damage in UHPC. In this study, the finite element program ABAQUS was used to simulate the push-out tests in which the geometric and material nonlinearity, material damage and complicated contact interaction were taken into account.

2.1 Description of experimental results

Before establishing the FE model, experiment details and results conducted by Wang *et al.* (2019) and Qi *et al.* (2017b) are briefly introduced hereafter. Totally, four specimens including two UHPC specimens and two NSC specimens were selected to verify the following established FE model. Fig. 1 shows the details and parameters of all test specimens. Two of the specimens (UHPC22 and UHPC30) were made by UHPC and the other two specimens (TJ2 and TJ3) were made by NSC. The compressive strengths of NSC and UHPC were 56.4 MPa and 124.0 MPa, respectively. The diameter of the studs in UHPC22 and UHPC30 was 22 mm and 30 mm, respectively. In the TJ2 and TJ3, the shear studs were pre-damaged to the damage degree of 12.8% and 36.6%. The interfacial slips were measured using dial indicator and the cracks were identified and marked at each loading increment. Detailed information about the ingredients and properties of test materials can be found in Wang *et al.* (2019) and Qi *et al.* (2017b).

All the specimens experienced shank failure. No cracks

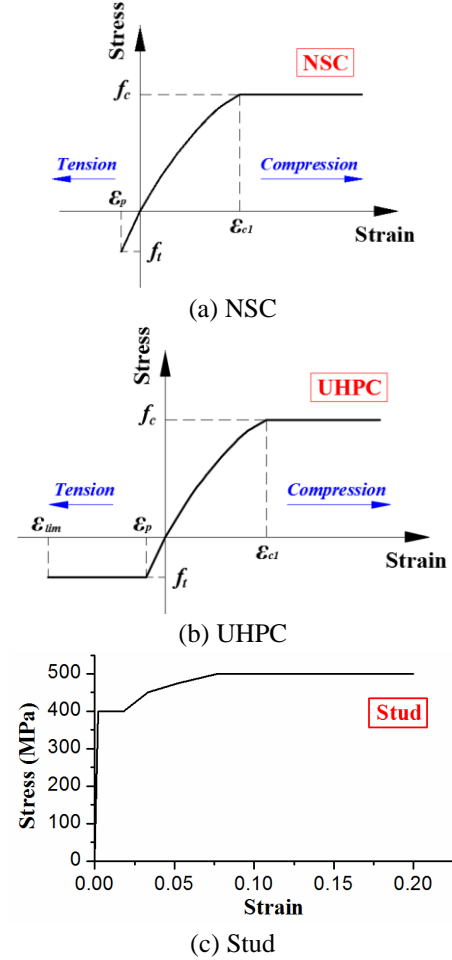


was found for the UHPC specimens while extensive splitting cracks on concrete slab were detected for the NSC specimens, indicating good resistance of UHPC on the transversal high splitting force beneath the headed studs. The load-slip curves of the test specimens are plotted in Fig. 2. Three different stages are observed in the load-slip curves: linear elastic stage, plastic stage and ultimate stage. The slip was very small in the elastic stage and the load-slip response remained a linear behavior. However, the slip increased significantly in the plastic stage and the stud shear stiffness decreased continuously. At the ultimate stage, the slip increased rapidly with a slight increment of the applied load and the studs were eventually fractured. Increasing the stud diameter can significantly improve the shear strength. The shear strength of 30 mm stud was 75% higher than that of 22 mm stud in UHPC. Therefore, large studs match well with UHPC. For NSC specimens, reductions of 0.7% and 13.4% in the shear stiffness corresponds to the shear stiffness at a slip of 2 mm as suggested by Qi *et al.* (2017b) were observed when damage degrees were 12.8% and 36.6%, respectively.

2.2 Material model and properties

Multilinear isotropic hardening model was selected for the studs and concrete while bilinear isotropic hardening model was adopted for the steel beam. Fig. 3 shows the material constitutive models. The stress-strain relationship for the studs was based on the experimental tensile test and characterized by a multilinear model. For compression, concrete was treated as an elastic-plastic material and the descending stage was neglected because the local crushing of concrete underneath the stud shank is not the focus of this study. As a result, the stress-strain relationship of concrete can be expressed as

$$\frac{\sigma_c}{f_c} = \frac{k\eta - \eta^2}{1 + (k-2)\eta} \quad (1)$$



where σ_c is the compressive stress in the concrete; f_c is the concrete compressive strength; $\eta = \epsilon_c / \epsilon_{c1}$; ϵ_{c1} is the strain at maximum compressive stress and ϵ_c is the strain in the concrete; $k = 1.05 E_c \times \epsilon_{c1} / f_c$ according to EC2 (ECS 2004); E_c is the elastic modulus of concrete.

For tension, different curves were adopted for UHPC and NSC due to the difference in their tensile behavior. NSC was treated as a linear elastic material up to the tensile strength while UHPC was modeled as an elastic-plastic material (Meng and Khayat 2016, Meng *et al.* 2018). The tensile stress-strain relationship was expressed by

$$\sigma_t = \begin{cases} E_c \epsilon_t & \epsilon_t \leq \epsilon_p \\ f_t & \epsilon_t > \epsilon_p \end{cases} \quad \text{for UHPC} \quad (2a)$$

$$\sigma_t = E_c \epsilon_t \quad \text{for NSC} \quad (2b)$$

where σ_t and ϵ_t are the tensile stress and strain in the concrete; f_t is the tensile strength; ϵ_p is the strain at maximum tensile stress and ϵ_{lim} is the ultimate strain.

2.3 Model establishment

In light of the symmetry of the geometrical dimensions, boundary conditions and loading mechanisms, half of the test specimens were simulated with the consideration of

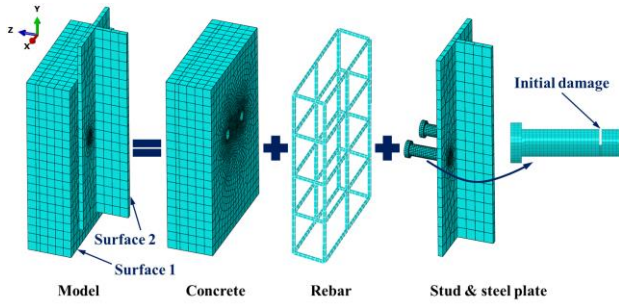


Fig. 4 FE model

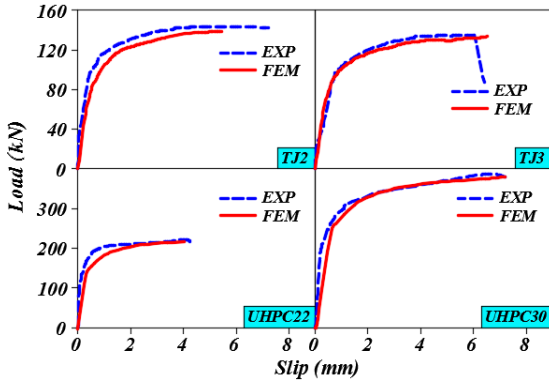


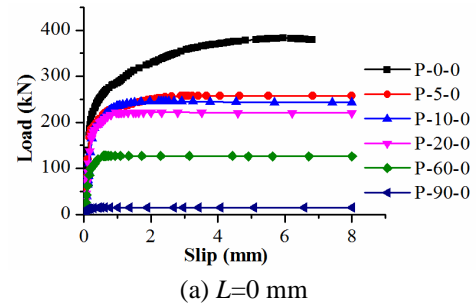
Fig. 5 Comparison of the FE predicted and experimental load-slip curves

computational efficiencies. As shown in Fig. 4, four parts, including concrete, rebar, studs and steel plate, were assembled to establish the FE model based on mechanical symmetrical regulation. In the FE model, three-dimensional eight node reduced integration element (C3D8R) was used to simulate concrete, studs and steel plate. Three-dimensional two-node truss element (T3D2) was introduced to simulate the embedded reinforcements. The penalty contact method was used to capture potential relative sliding at the contact surfaces between steel flanges and concrete slabs and between stud shear connectors and surrounding concrete. As recommended by Xu *et al.* (2012) and Qi *et al.* (2017b), the coefficient of friction between the interlayer faces was assumed to be 0.3. Perfect bond between concrete and rebars was applied using the embedded method.

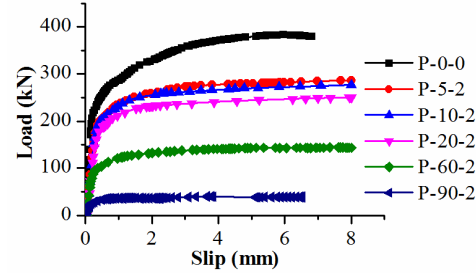
Concerning the model's boundary condition, the bottom concrete surface (surface 1) was restrained in all three directions. The symmetry boundary condition was applied to the steel beam web surface (surface 2), meaning that all nodes located on this surface were restrained along the X axis. The loading surface of the steel beam is also shown in Fig. 4. In order to prevent a dramatic increase in the kinematic energy, an optimum loading rate of 0.02 mm/s was adopted as recommended by Qi *et al.* (2017b).

2.4 Model verification

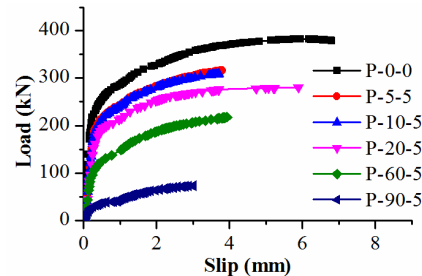
Fig. 5 shows the comparison of the analyzed load-slip curves obtained by the numerical simulation and the experimental tests for each specimen. The numerical results agreed well with the test results for both studs in UHPC and



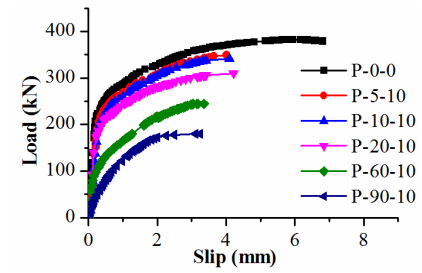
(a) $L=0$ mm



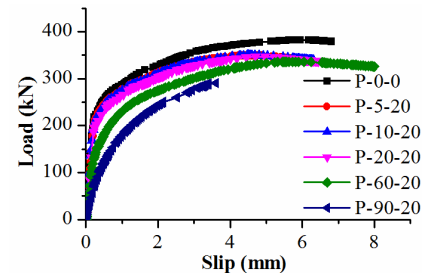
(b) $L=2$ mm



(c) $L=5$ mm



(d) $L=10$ mm



(e) $L=20$ mm

Fig. 6 Effect of damage degree on the load-slip curves

studs with initial damage in NSC, verifying the reliability of the FE model. The small differences might be attributed to the differences between the real and assumed material constitution, contact interaction and boundary condition. Therefore, it is believed that the proposed FE model has sufficient accuracy and reliability to simulate the push-out tests and to conduct the following parametric study.

Table 1 FE analysis parameters and results

Specimen	η (%)	L (mm)	P_u (kN)	ζ (%)	S_u (mm)	S_{max} (mm)	k (kN/mm)
P-0-0	-	-	382.5	0	6.0	6.7	164.1
P-5-0	5	0	280.4	-27	3.1	8	124.7
P-10-0	10	0	266.7	-30	2.2	8	122.6
P-20-0	20	0	241.2	-37	1.8	8	110.9
P-60-0	60	0	127.2	-67	0.7	8	63.4
P-90-0	90	0	14.9	-96	8	8	7.4
P-5-2	5	2	286.0	-25	8	8	129.7
P-10-2	10	2	276.6	-28	8	8	127.5
P-20-2	20	2	250.3	-35	8	8	116.3
P-60-2	60	2	144.1	-62	7.6	8	66.1
P-90-2	90	2	39.8	-90	3.8	6.5	18.2
P-5-5	5	5	315.7	-17	3.8	3.8	141.1
P-10-5	10	5	308.4	-19	3.7	3.7	140.3
P-20-5	20	5	280.5	-27	5.9	5.9	126.6
P-60-5	60	5	217.5	-43	3.9	3.9	93.7
P-90-5	90	5	72.9	-81	3.0	3.0	32.0
P-5-10	5	10	349.2	-9	4.0	4.0	153.9
P-10-10	10	10	341.6	-11	4.1	4.1	152.0
P-20-10	20	10	310.0	-19	4.2	4.2	140.7
P-60-10	60	10	244.8	-36	3.4	3.4	108.5
P-90-10	90	10	180.1	-53	3.3	3.3	86.0
P-5-20	5	20	349.5	-9	4.5	5.8	156.0
P-10-20	10	20	349.6	-9	4.7	6.3	155.0
P-20-20	20	20	347.1	-9	5.0	6.4	151.4
P-60-20	60	20	336.4	-12	5.8	8	137.5
P-90-20	90	20	290.2	-24	3.6	3.6	122.1

Note: P = push-out test with one damage location; PD = push-out with double damage locations; L = damage location (distance from the root to the location of the damage); P_u = ultimate strength per stud; S_u = interfacial slip corresponding to peak load; S_{max} = ultimate slip; ζ = Dropping rate in the maximum shear strength to that of specimen P-0-0; k = shear stiffness at the 2 mm relative slip.

3. Numerical analysis results

3.1 Specimens and parameters

A numerical investigation was conducted using the verified FE model to study the effect of initial damage on the static behavior of stud shear connectors embedded in UHPC. UHPC30 (renamed as P-0-0) was adopted as the reference specimen. Two parameters including damage degree and damage location were selected for the numerical analysis. The damage degree is defined as the reduction in the stud shank area and the damage location is the distance from the damaged section to the root of the shank. Six damage degrees, which were 0%, 5%, 10%, 20%, 60% and 90%, were selected because severe damage (large damage degree) would not occur usually. Damage locations of 0, 2, 5, 10 and 20 mm (i.e., the distance from the root to the location of the damage) were investigated simultaneously because the damage to shear stud usually take place close to the root in practice. The specimen ID was designated as "Push-out (P)-damage degree-damage location". For example, specimen P-5-2 represents a push-out specimen with 5% damage on the section 2 mm from stud root. The results from the analysis on a total of 26 specimens were summarized in Table 1.

3.2 Effect of damage degree

Fig. 6 shows the load-slip curves of each FE push-out specimens listed in Table 1. As the damage degree increased, the shear strength decreased significantly. This could be explained by the increment in stud shear area and stud shank failure mode, in which the stud strength and stud area dominants the shear strength. Fig. 7 illustrates the effect of damage degree on the shear strength and shear stiffness of studs. The reduction in shear strength increased as the damage degree increased, as shown in Fig. 7(a). As shown in Table 1, for specimens with stud root damage, the decrements in shear strength compared to the reference specimen were from 27% to 96% as the damage degree increased from 5% to 90%. For specimens with damage at the section 20 mm from stud root, the decrements in shear strength compared to the standard specimen were from 9% to 24% as the damage degree increased from 5% to 90%. This phenomenon indicated that the decrement in shear strength of specimens with initial damage compared to the reference specimen (i.e. un-damaged specimen) becomes more significant for the specimens with shorter damage locations. It is interesting to note that shear strength is also shown to be insensitive to the damage degree when the damage location is $2/3d$, where d is the shank diameter,

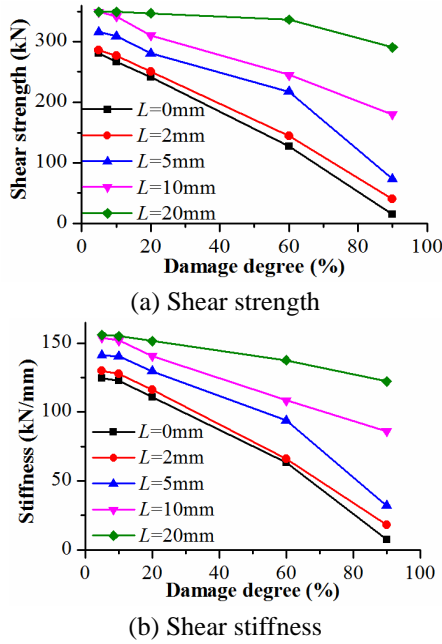


Fig. 7 Effect of damage degree on the shear strength and stiffness of studs

from the stud root even if the stud has experienced a significant reduction in area. Therefore, it is believed that damage to the stud could be neglected when the distance from the damage location to root is larger than $2/3d$.

Shear stiffness is an important characteristic for the stud shear connectors. As suggested by Qi *et al.* (2017b), the shear stiffness could be calculated by the secant slope of load-slip curve at a relative of 2 mm. The calculation result of the specimens shear stiffness is plotted in Fig. 7(b). Generally, the shear stiffness decreased as the damage degree increased. The shear stiffness decreased linearly when the damage location is far away from the stud root whereas the shear stiffness decreased non-linearly when the damage location is near the stud root.

Fig. 8 shows the Von Mises stresses of all specimens listed in Table 1 at ultimate state. It can be seen that stud shank failure occurred in all specimens. As the damage degree increased, the stress concentration moved toward the remaining area of the damaged section, indicating a fact that the efficient shear resistance area in a stud reduced. As a result, the shear strength decreased due to the damage on a stud.

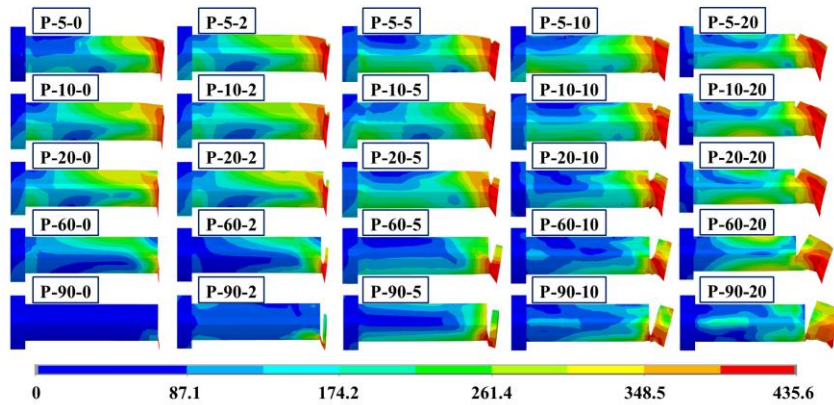


Fig. 8 Von Mises stresses of studs at ultimate state

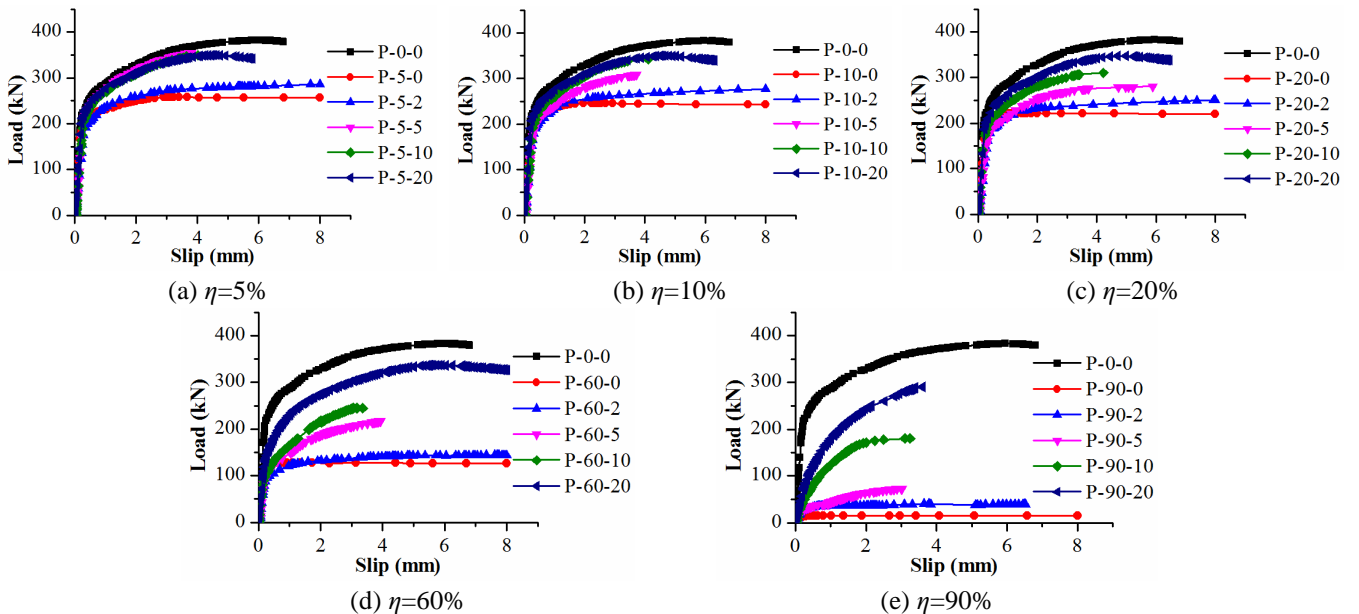


Fig. 9 Effect of damage location on the load-slip curves

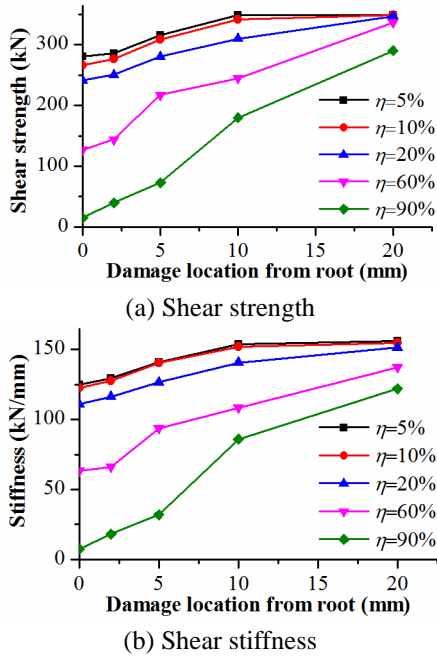


Fig. 10 Effect of damage location on the shear strength and shear stiffness of studs

3.3 Effect of damage location

The effect of damage location on the shear behavior of studs is shown in Fig. 9 and Fig. 10. Fig. 9 plots the load-slip curves of all specimens with different damage location under a certain damage degree. As the damage location moved away from the stud root, the reduction on shear strength decreased, especially for specimens with high damage degree. It can be seen from Fig. 10(a) that the shear strength reduction decreased dramatically for specimens with high damage degree compared to those of specimens with low damage degree. This is because the influence of damage degree on the shear strength is significant when the damage location is near stud root. Similarly, the shear stiffness reduction decreased as the distance of damage location from stud root increased, and this trend becomes more significant for specimens with high damage degree, as shown in Fig. 10(b). This phenomenon could be explained as the change in the Von Mises stresses of studs at ultimate state. As shown in Fig. 8, one can find that when the distance of damage location from stud root increased, a larger stud area could be engaged in resisting shear force and the failure section becomes inclined, which is not perpendicular to the stud height direction, resulting in increasing in the shear strength and shear stiffness.

4. Strength prediction on studs with initial damage

Initial damage on studs induced by corrosion, fatigue, mechanical defects, weld defects, etc. weaken the shear strength. Therefore, strength evaluation on studs with damage is necessary. Practice reveals that most damage occurs at the region close to the stud root. As shown in Fig. 10, although the reduction of shear strength decreased as the

damage location from stud root increased, it is believed that using the shear strength calculated with root damage as the ultimate capacity is reasonable because this value is a conservative and safe estimation for different damage locations under a given damage degree.

As indicated in the previous parametric study, initial damage of a stud would result in a reduction in its shear strength and tend to be more prominent for those with larger damage degree. However, the current specifications and existing theoretical calculation methods do not consider the influence of the initial damage on the stud shear strength. Consequently, a reasonable calculation method on the stud shear strength reduction should be proposed. In this study, a reduction factor is introduced to consider the effect of the damage degree on the shear strength of the stud. Thus, the design shear strength of a stud can be expressed as follows

$$P_{Rd} = K \times \min(P_{stud}, P_{concrete}) \quad (3)$$

where P_{stud} and $P_{concrete}$ are the shear strength dominated by “stud failure” and “concrete failure”, respectively, which could be calculated using the expression of an undamaged stud. How to determine the formula for the reduction factor K remains a critical problem.

Two different approaches for stud shear strength for the initial damage of a stud are proposed. According to intuitive judgment, it seems that a linear relationship between the shear strength reduction factor and the damage degree should be reasonable. Thus, this speculation can be used as one principle of judgment on the effect of the initial damage on the shear strength. However, a nonlinear relationship between the shear strength reduction factor and the damage degree may occur because the stress state of a damaged stud differs from that of an integrated stud. It is deduced that the reduction factor satisfies a linear relationship with a nominal diameter of the remaining stud area after transferring it to an intact circle.

4.1 Reduction factor K_1 – approach 1

A linear relationship between reduction factor K_1 and η is assumed based on the fact that all the design codes adopt linear relationship between shear strength and the sectional area of the studs. The failure mode of a stud could be determined by Eurocode 4 (ESC 2005). For concrete failure, K_1 can be determined by

$$K_1 = \begin{cases} 1 - \frac{\eta - K_c}{1 - K_c} & \eta \geq K_c \\ 1 & \eta < K_c \end{cases} \quad \text{when } f_{ck} < 4.69 f_u^2 / \alpha^2 E_{cm} \quad (4a)$$

For stud failure, K_1 is expressed as

$$K_1 = 1 - \eta \quad \text{when } f_{ck} \geq 4.69 f_u^2 / \alpha^2 E_{cm} \quad (4b)$$

where f_{ck} is concrete cylinders compressive strength; E_{cm} is the Young's modulus of the concrete; f_u is the stud ultimate tensile strength; $\alpha = 0.2(h_{sc}/d + 1) \leq 1$, where d is the stud diameter; h_{sc} is the overall height of a stud; and K_c is the critical damage degree and can be calculated by

$$K_c = 1 - 0.46 \alpha \sqrt{f_{ck} E_{cm}} / f_u \quad (5)$$

Table 2 Comparison of calculated results and FE results

Specimen	η	P_u (kN)	Eurocode 4		AASHTO		GB50017-2003	
			P_1 (kN)	P_2 (kN)	P_1 (kN)	P_2 (kN)	P_1 (kN)	P_2 (kN)
P-0-0	0	382.5	246.3	246.3	307.9	307.9	266.2	266.2
P-5-0	5	280.4	234.0	240.1	292.5	300.1	252.9	259.4
P-10-0	10	266.7	221.7	233.7	277.1	292.1	239.6	252.5
P-20-0	20	241.2	197.1	220.3	246.3	275.4	212.9	238.1
P-60-0	60	127.2	98.5	155.8	123.2	194.7	106.5	168.4
P-90-0	90	14.9	24.6	77.9	30.8	97.4	26.6	84.2

Note: P_1 and P_2 represent the predicted shear strength calculated using approach 1 and approach 2, respectively.

4.2 Reduction factor K_2 – approach 2

In approach 2, a quadratic relationship is assumed between the shear strength and the stud area, resulting in a linear relationship between the reduction factor and the stud nominal diameter. Thus, for concrete failure, the reduction factor K_2 is determined by

$$K_2 = \begin{cases} 1 - \sqrt{\frac{\eta - K_c}{1 - K_c}} & \eta \geq K_c \\ 1 & \eta < K_c \end{cases} \quad \text{when } f_{ck} < 4.69f_u^2 / \alpha^2 E_{cm} \quad (6a)$$

For stud failure, the reduction factor K_2 is calculated by

$$K_2 = \sqrt{1 - \eta} \quad \text{when } f_{ck} \geq 4.69f_u^2 / \alpha^2 E_{cm} \quad (6b)$$

4.3 Verification

In order to verify the proposed reduction factor, the shear strengths of studs with different damage degree on the stud root are estimated based on the current design specifications (ESC 2005, AASHTO LRFD 2014, GB50017-2003). The comparison results are shown in Table 2. It can be seen that the shear strength calculated by approach 1 yields a more accurate and safe prediction than that of approach 2, which is contrary to the results obtained by Qi *et al.* (2017b). This different result can be explained as follow. In normal strength concrete, concrete usually crush extensively at failure. Thus, the shear strength calculated by multiplying stud area and ultimate strength would over-estimate the shear strength. As a result, using approach 2 would produce a more accurate prediction. However, such situation would change for a UHPC slab. As indicated by Wang *et al.* (2019), only a small area of concrete is sheared off from the UHPC slab. Therefore, the concrete contribution is not significant compared to the case in normal strength concrete. That is to say, approach 1 is more suitable for the stud shear strength prediction in UHPC.

5. Conclusions

A numerical and theoretical investigation on the static behavior of stud shear connectors with initial damage

embedded in UHPC was conducted under the parameters of damage degree and damage location. Based on the analysis results, the following conclusions can be drawn:

- The shear strength of a stud is shown to be insensitive to the damage degree when the damage location is $2/3d$ (d is the stud diameter) from the stud root even if the stud has experienced a significant reduction in area.
- When the distance of damage location from stud root increased, a larger stud area would be engaged in resisting shear force and the failure section becomes inclined, which is not perpendicular to the stud height direction, resulting in a less reduction in the shear strength and shear stiffness.
- A new concept of reduction factor was proposed to consider the reduction of the shear strength of the damaged stud. Two approaches were evaluated to determine the expression of the reduction factor. The reduction factor was assumed to satisfy a linear relationship with the damage degree in the first approach while the reduction factor in the second approach was assumed to satisfy a quadratic relationship with the damage degree, corresponding to a linear relationship with the nominal stud diameter.
- Comparison of calculated results and FE results showed that the proposed methods could be used to predict the shear strength of a stud with initial damage. The first method is more suitable for use in engineering design.
- Although the study offers an alternative way in understanding the shear behavior of stud shear connectors with initial damage embedded in UHPC, experimental verification is needed in the future study.

Acknowledgments

This study was supported by the National Natural Science Foundation of China (Grant No. 51908122), the National Key R&D Plan (2017YFC07034), “Zhishan” Scholars Programs of Southeast University, the Technology R&D Project of China Communications Construction Company (Grant No. 2018-ZJKJ-02), and the Fundamental Research Funds for the Central Universities. The financial supports are gratefully appreciated.

References

- AASHTO (2014), Bridge Design Specifications, American Association of State Highway and Transportation Officials, Washington, DC, USA.
- Cao, J., Shao, X., Deng, L. and Gan, Y. (2017), “Static and fatigue behavior of short-headed studs embedded in a thin ultrahigh-performance concrete layer”, *J. Bridge Eng.*, **22**(5), 04017005. [https://doi.org/10.1061/\(ASCE\)BE.1943-5592.0001031](https://doi.org/10.1061/(ASCE)BE.1943-5592.0001031).
- De Larrard, F. and Sedran, T. (1994), “Optimization of ultra-high-performance concrete by the use of a packing model”, *Cement Concrete Res.*, **24**(6), 997-1009. [https://doi.org/10.1016/0008-8846\(94\)90022-1](https://doi.org/10.1016/0008-8846(94)90022-1).
- ECS (European Committee for Standardization) (2004), Eurocode 2: Design of Concrete Structures-Part 1-1: General Rules and Rules for Buildings (EN 1992-1-1), Brussels, Belgium.

- ECS (European Committee for Standardization) (2005), Eurocode 4: Design of Composite Steel and Concrete Structures, Part 1-1: General Rules and Rules for Buildings (EN 1994-1-1), Brussels, Belgium.
- GB50017-2003 (2003), Code for Design of Steel Structures, Beijing, China.
- Kim, J.S., Kwark, J., Joh, C., Yoo, S.W. and Lee, K.C. (2015), "Headed stud shear connector for thin ultrahigh-performance concrete bridge deck", *J. Constr. Steel Res.*, **108**, 23-30. <https://doi.org/10.1016/j.jcsr.2015.02.001>.
- Kruszewski, D., Wille, K. and Zaghi A.E. (2018), "Push-out behavior of headed shear studs welded on thin plates and embedded in UHPC", *Eng. Struct.*, **173**, 429-441. <https://doi.org/10.1016/j.engstruct.2018.07.013>.
- Liu, Y., Zhang, Q., Meng, W., Bao, Y. and Bu, Y. (2019), "Transverse fatigue behaviour of steel-UHPC composite deck with large-size U-ribs", *Eng. Struct.*, **180**, 388-399. <https://doi.org/10.1016/j.engstruct.2018.11.057>.
- Meng, W. and Khayat, K.H. (2016), "Mechanical properties of ultra-high-performance concrete enhanced with graphite nanoplatelets and carbon nanofibers", *Compos. Part B-Eng.*, **107**, 113-122. <https://doi.org/10.1016/j.compositesb.2016.09.069>.
- Meng, W., Khayat, K.H. and Bao, Y. (2018), "Flexural behaviors of fiber-reinforced polymer fabric reinforced ultra-high-performance concrete panels", *Cement Concrete Compos.*, **93**, 43-53. <https://doi.org/10.1016/j.cemconcomp.2018.06.012>.
- Mosaberpanah, M.A. and Eren, O. (2017), "Effect of quartz powder, quartz sand and water curing regimes on mechanical properties of UHPC using response surface modeling", *Adv. Concrete Constr.*, **5**(5), 481-492. <https://doi.org/10.12989/acc.2017.5.5.481>.
- Oehlers, D.J. and Park, S.M. (1992), "Shear connectors in composite beams with longitudinally cracked slabs", *J. Struct. Eng.*, **118**(8), 2004-2022. [https://doi.org/10.1061/\(ASCE\)0733-9445\(1992\)118:8\(2004\)](https://doi.org/10.1061/(ASCE)0733-9445(1992)118:8(2004)).
- Qi, J., Hu, Y., Wang, J. and Li, W. (2019a), "Behavior and strength of headed stud shear connectors in ultra-high performance concrete of composite bridges", *Front. Struct. Civil Eng.*, **13**(5), <https://doi.org/10.1007/s11709-019-0542-6>.
- Qi, J., Ma, Z.J. and Wang, J. (2017a), "Shear strength of UHPFRC beams: mesoscale fiber-matrix discrete model", *J. Struct. Eng.*, **143**(4), 04016209. [https://doi.org/10.1061/\(ASCE\)ST.1943-541X.0001701](https://doi.org/10.1061/(ASCE)ST.1943-541X.0001701).
- Qi, J., Wang, J. and Feng, Y. (2019b), "Shear performance of an innovative UHPFRC deck of composite bridge with coarse aggregate", *Adv. Concrete Constr.*, **7**(4), 219-229. <https://doi.org/10.12989/acc.2019.7.4.219>.
- Qi, J., Wang, J. and Ma, Z.J. (2018a), "Flexural response of high-strength steel-ultra-high-performance fiber reinforced concrete beams based on a mesoscale constitutive model: Experiment and theory", *Struct. Concrete*, **19**(3), 719-734. <https://doi.org/10.1002/suco.201700043>.
- Qi, J., Wang, J., Li, M. and Chen, L. (2017b), "Shear strength of stud shear connectors with initial damage: experiment, FEM model and theoretical formulation", *Steel Compos. Struct.*, **25**(1), 79-92. <https://doi.org/10.12989/scs.2017.25.1.079>.
- Qi, J., Wu, Z., Ma, Z.J. and Wang, J. (2018b), "Pullout behavior of straight and hooked-end steel fibers in UHPC matrix with various embedded angles", *Constr. Build. Mater.*, **191**, 764-774. <https://doi.org/10.1016/j.conbuildmat.2018.10.067>.
- Rauscher, S. and Hegger, J. (2008), "Modern composite structures made of high performance materials" *Proc., Composite Construction in Steel and Concrete Conf.*, VI, Devil's Thumb Ranch, Tabernash, CO, ASCE, Reston, VA.
- Shao, X., Qu, W., Cao, J. and Yao, Y. (2018), "Static and fatigue properties of the steel-UHPC lightweight composite bridge deck with large U ribs", *J. Constr. Steel Res.*, **148**, 491-507. <https://doi.org/10.1016/j.jcsr.2018.05.011>.
- Sharma, R. and Bansal, P.P. (2019), "Efficacy of supplementary cementitious material and hybrid fiber to develop the ultra high performance hybrid fiber reinforced concrete", *Adv. Concrete Constr.*, **8**(1), 21-31. <https://doi.org/10.12989/acc.2019.8.1.021>.
- Wang, J., Guo, J., Jia, L., Chen, S. and Dong, Y. (2017), "Push-out tests of demountable headed stud shear connectors in steel-UHPC composite structures", *Compos. Struct.*, **170**, 69-79. <https://doi.org/10.1016/j.compstruct.2017.03.004>.
- Wang, J., Qi, J., Teng, T., Xu, Q. and Xiu, H. (2019), "Static behavior of large stud shear connectors in steel-UHPC composite structures", *Eng. Struct.*, **178**, 534-542. <https://doi.org/10.1016/j.engstruct.2018.07.058>.
- Xu, C. and Sugiura, K. (2013), "Parametric push-out analysis on group studs shear connector under effect of bending-induced concrete cracks", *J. Constr. Steel Res.*, **89**, 86-97. <https://doi.org/10.1016/j.jcsr.2013.06.011>.
- Xu, C., Sugiura, K., Wu, C. and Su, Q. (2012), "Parametrical static analysis on group studs with typical push-out tests", *J. Constr. Steel Res.*, **72**, 84-96. <https://doi.org/10.1016/j.jcsr.2011.10.029>.

CC